# Direct Drive Uniformity Calculations for a Future High Gain Laser Facility

Sara C. Davies

Pittsford Sutherland High School

Pittsford, NY

Advisor: Dr. R. Stephen Craxton

Laboratory for Laser Energetics

University of Rochester

Rochester, NY

December 2023

**Abstract**

This work investigates the optimization of uniformity for direct drive experiments on a possible future laser facility larger than the National Ignition Facility (NIF). The NIF has 48 groups of 4 beams, or quads. The proposed facility has 96 quads. A key feature of the facility is that it can perform both direct and indirect drive. Indirect drive will use octahedral hohlraums, which promise greater uniformity than the cylindrical hohlraums used on the NIF. The 2-D hydrodynamic code *SAGE* was applied to evaluate beam repointing for direct drive. The optimum repointing obtained maintains all beam repointings below 14.1° and gives a root mean square nonuniformity of 0.41%. These results show that the optimized design promises highly uniform direct drive implosions on a facility also capable of highly uniform indirect drive.

## I Introduction

Nuclear fusion promises a long-lasting source of clean energy. One approach to fusion uses laser beams to heat a spherical capsule that contains fuel made of deuterium (D) and tritium (T), two isotopes of hydrogen. As the exterior of the capsule is heated to high temperatures it turns into an expanding plasma, thus exerting an inward pressure on the fuel. The compressed fuel can reach densities and temperatures far higher than those found anywhere else on the Earth. The high temperature of the fuel allows the positively charged D and T nuclei to overcome the electrostatic repulsion forces, allowing fusion to occur, while the high density ensures that enough fusion reactions occur before the fuel expands and cools. DT fusion forms a helium nucleus, or alpha particle, and releases a large amount of energy, mostly in the form of energetic neutrons. The helium nucleus can further heat the compressed fuel if the density and radius of the fuel are sufficient, reducing the energy required from the laser beams.

There are two approaches to laser-driven fusion, direct and indirect drive (Fig. 1). In direct drive, laser beams directly irradiate the capsule. For indirect drive, the capsule is placed in a case, known as a hohlraum, made of a high-Z material, typically gold. The laser beams enter the hohlraum through laser entrance holes and deposit energy on the hohlraum walls. The walls then emit x rays, which irradiate the capsule. Indirect drive is less energy efficient than direct drive as only a fraction of the laser power, 10-20%, is absorbed by the capsule. Indirect drive is, however, less sensitive to small imperfections in the laser beams.

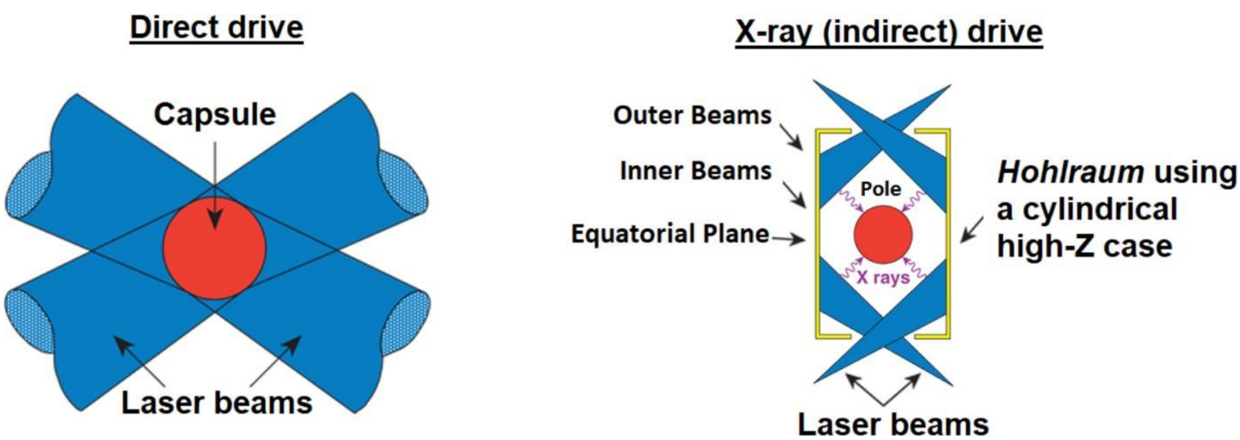


Figure 1: *The two main approaches to laser-driven fusion, direct and indirect drive. The model of indirect drive depicts a cross-section of a cylindrical hohlraum. From Ref. 1*

Regardless of the approach used, it is essential to obtain high levels of irradiation uniformity on the capsule [2]. The National Ignition Facility (NIF), dedicated to indirect drive, currently uses cylindrical hohlraums, which make it difficult to implode the spherical fuel capsules uniformly. With heroic efforts, Livermore have been able to obtain implosions with very good uniformity. During the implosion, material that ablates from the hohlraum wall makes it difficult for the inner beams to reach the equator of the hohlraum, reducing the drive on the equator.

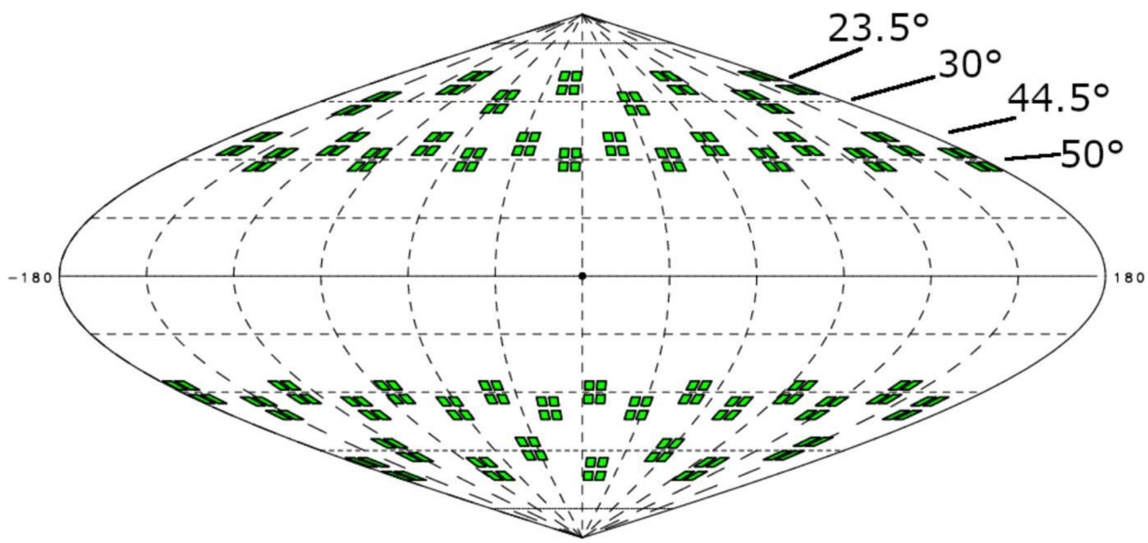


Figure 2: *The locations of laser beam ports on the NIF target chamber, indicated in green, are grouped into 48 quads of four beams each. From Ref. 1*

Due to the NIF's target chamber design, symmetrical direct drive is impractical. The NIF beam ports are specifically designed to perform indirect drive experiments with cylindrical hohlraums. The beam ports are arranged in four rings in each hemisphere with a total of 48 quads, which are groups of four beams (Fig. 2). If the beams are pointed at the center of the capsule for direct drive experiments, the equatorial regions of the capsule are underdriven compared to the poles. To perform direct drive experiments on the NIF the beams need to be repointed towards the equator. Some of the beams need to be repointed by as much as 35° [3, 4]. When the beams are repointed by such a large angle, the energy from the beams refracts around the edge of the capsule, reducing absorption. Also, the distribution of energy around the surface of the capsule changes as the capsule implodes, limiting the convergence that can be achieved. Therefore, the NIF is unsuitable for uniform high-convergence direct drive implosions.

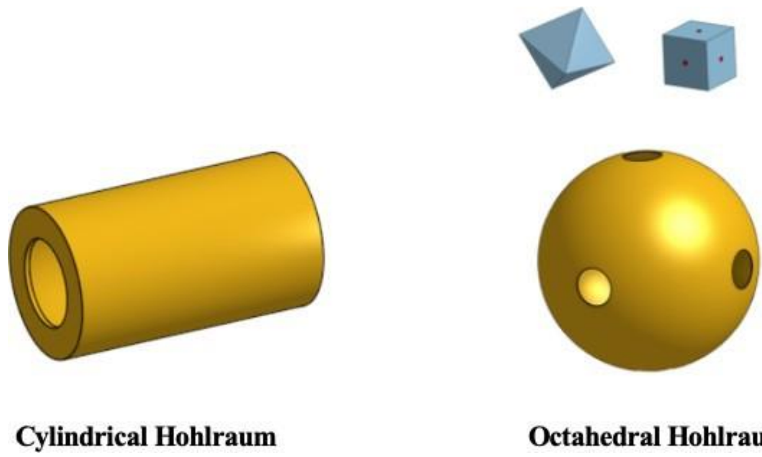


Figure 3: *Comparison between cylindrical and octahedral hohlraums. The holes in the hohlraums represent laser entrance holes. The octahedral hohlraum has six laser entrance holes, corresponding to the six vertices of a regular octahedron or faces of a cube. From Ref. 1*

Octahedral hohlraums have been proposed as more uniform alternatives to cylindrical hohlraums, using 48 quads [5, 6, 7]. As shown in Fig. 3, the octahedral hohlraum has six laser entrance holes that correspond to the six vertices of an octahedron. The geometry of the octahedral hohlraum provides greater uniformity than cylindrical hohlraums. However, the NIF cannot use octahedral hohlraums as the NIF does not match the cubic symmetry needed for them.

Here, a higher energy, 96-quad laser facility is proposed to drive an octahedral hohlraum (Fig. 3) to achieve higher gain than the 48-quad NIF. The proposed facility would have twice as many beams as the NIF. Unlike the NIF, the proposed facility would be capable of driving highly symmetric, high-convergence implosions using both direct and indirect drive. The proposed facility extends previous work that investigated achieving both direct and indirect drive on a 48-quad system [1] to a 96-quad system.

## II Layout of the 96-Quad System

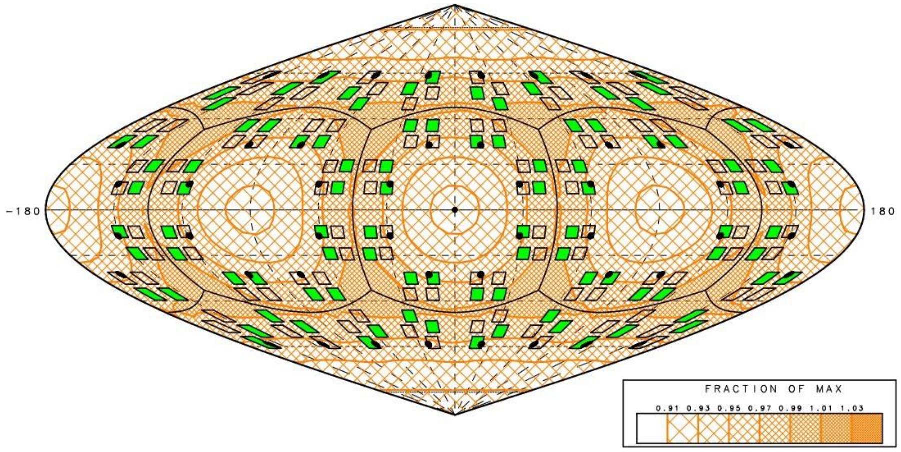


Figure 4: *Sinusoidal projection of the proposed 96-quad system. Green squares are beam ports. Black dots are the "ideal" aim points on a direct drive capsule. Open black squares represent the beam dumps on the opposite side of the target chamber. The curved black lines correspond to the edges of the cube. The contours give the relative irradiation intensity on the capsule when the beams are pointed at the closest ideal aim points. The lowest contour level drawn is 93% of maximum and the root mean square (RMS) intensity variation on the capsule surface is 2.26%.*

Figure 4 shows a projection of the proposed system, with the green squares indicating the 96 quads and the open squares the beam dumps on the opposite side of the target chamber. (Note that in Fig. 2, each green square represents a single beam.)

Like the NIF, the 96-quad system has non-opposed beams so that if a beam misses the target it cannot pass through the opposing port and damage the optics in the IR portion of the laser system. Instead, beam dumps are provided on the chamber wall. The beam dumps are also required to absorb the unconverted infrared and second-harmonic light from the frequency conversion process. The geometry of the 96-quad system allows for good diagnostic access, with large areas available at the six faces and eight corners of the cube. However, there are downsides to the 96-quad system's layout. The non-opposed beams make beam repointings for direct drive more difficult. Non-opposed beams also require double the solid angle for the beam dumps, complicating the design of the beam ports.

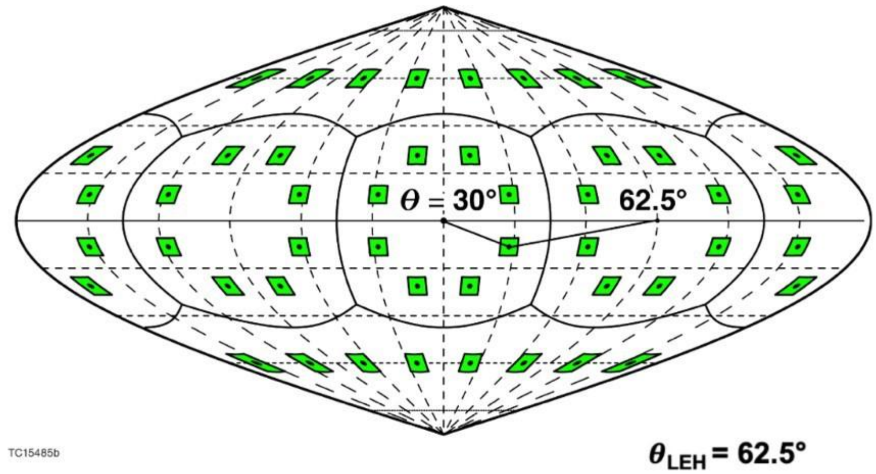


Figure 5: *Proposed 48-quad system from Refs. 8 and 9 with beams 30° from the centers of the cube faces. The black dots represent the "ideal" aim points. Figure from Refs. 10 and 11.*

Figure 4 also shows the "ideal" aim points (black dots), used as a starting point for the optimization of the 96-quad system. The ideal aim points are those proposed for a 48-quad Russian system [8, 9], illustrated in Figure 5. The 30° angle proposed in Refs. 8 and 9 provides excellent uniformity, as was independently confirmed in Refs. 10 and 11. For indirect drive using an octahedral hohlraum, all beams would enter the laser entrance hole on the adjacent face of the cube at 62.5° (although they could enter through the closest laser entrance hole at 30°).

For the *SAGE* simulation of Fig. 4, all beams are pointed at the ideal aim points. The contour levels show the time-integrated deposited energy. The simulation gives a root mean squared (RMS) intensity variation on the capsule surface of 2.26%. This RMS is high for efficient direct drive, considering that <1% is considered to be essential. Figure 4 shows that aiming at the ideal aim points results in too much deposition on the corners of the cube and too little at the centers of the faces of the cube. Simulations of a 48-quad system using these ideal aim points also resulted in a large RMS [10]. Thus it is necessary to repoint the beams to reduce the RMS nonuniformity below 1%.

## III Optimization of Beam Pointing

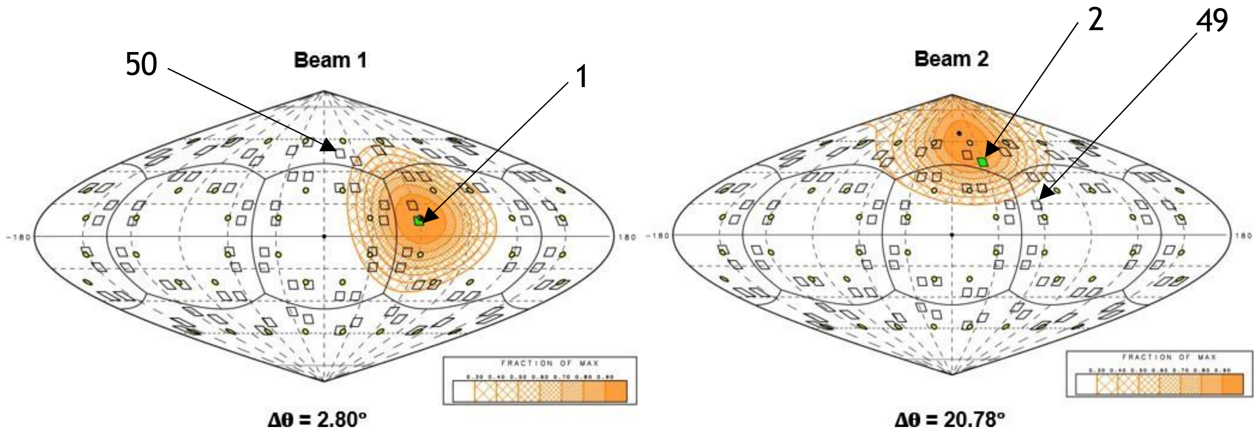


Figure 6: *Contour plots of the deposited laser energy on the capsule (as a fraction of the maximum) produced by beams 1 & 2 for the initial optimization. Left shows beam 1 and right shows beam 2, for the initial optimization. Beams/quads 1, 2, 49, and 50 are labeled by arrows. The yellow dots with black borders represent the ideal aim points. The black dots represent where beams 1 & 2 are actually pointed. Beam 1 is shifted 2.80° while beam 2 is shifted 20.78°.*

The first attempt at optimizing the beam repointings was based on individually optimizing four sets of beams, each set comprising 24 beams that have equivalent locations due to symmetry. Beams 1, 2, 49, and 50 in Fig. 6 represent the four sets. There are three equivalent locations on the cubic face that contains beam 1, obtained by 90° rotations, giving four equivalent beams per face or 24 equivalent beams total. Following Refs. 1 and 10, the beam locations are defined by the angle θ, representing the distance from the center of the face as shown in Fig. 5, and the azimuthal angle φ around the center of the face, measured counterclockwise relative to one of the axes. (For example, φ is 22.5° in Fig. 5.) In the proposed configuration, beam 1 is given by (θ=60°, φ=11°), beam 2 by (53°, 65.5°), beam 49 by (60°, 22.25°), and beam 50 by (53°, 77.75°). Each set is optimized by modeling just one of these four beams and rotating the deposited energy to the 23 equivalent locations.

Figure 6 depicts the cumulative deposited energy on the capsule for SAGE simulations of beams 1 and 2. The small yellow circles with black borders represent the ideal aim points and the small black dots show the actual aim points of beams 1 and 2 with the optimized repointings. Since beam 1 is located very close to an ideal aim point, the ideal and actual aim points are virtually the same. However, for beam 2, the actual aim point is moved beyond the ideal aim point (as in Ref. 10) so that the deposited energy pattern is centered on the ideal aim point. Similarly to the beam port locations, the aim-point locations are defined by two parameters ($\theta_{aim}$, $\varphi_{aim}$). The optimization is performed by varying these parameters.

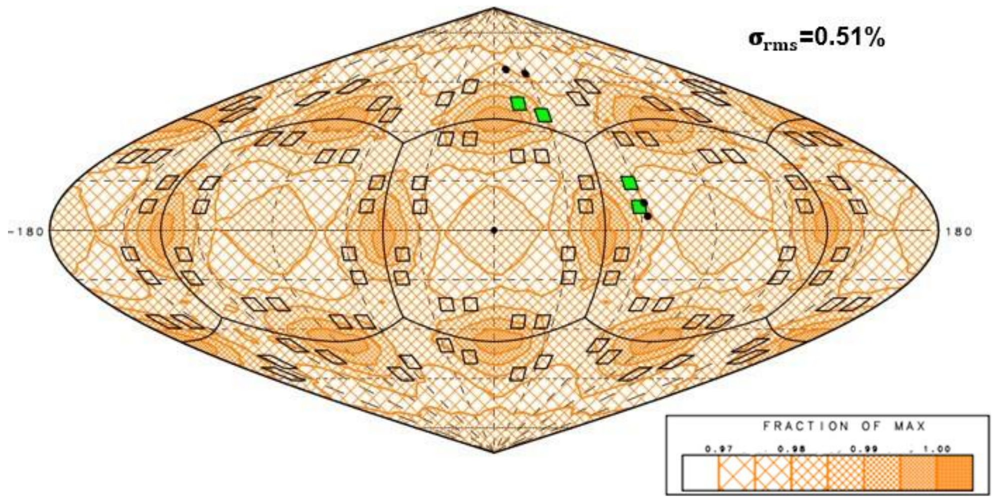


Figure 7: *Energy deposition pattern obtained by combining the patterns of four beams (1, 2, 49, 50) aimed past the ideal aim points as in Fig. 6 and symmetrizing them. The RMS nonuniformity is 0.51%.*

Figure 7 shows the result of combining the four beams (1, 2, 49, 50), each optimized individually as shown in Fig. 6, with the energy deposition pattern rotated to the 23 equivalent locations. The process of rotating the energy deposition patterns is known as symmetrizing. The pattern for each of the four beams was symmetrized individually to obtain the optimum pointing for each beam. The optimum pointings for each individual beam were then combined and the result symmetrized to produce the result shown in Fig. 7. By symmetrizing the energy deposition, it is possible to calculate the full energy deposition pattern modeling just four beams. The RMS nonuniformity significantly decreases from 2.26% to 0.51%.

Although the deposition pattern produced in Fig. 7 is far more uniform than the deposition pattern produced by aiming at the ideal aim points (Fig. 4), beam 2 requires repointing by 20.78° (measured around a great circle). This large repointing is not ideal because oblique incidence leads to lower absorption and can enhance energy loss from cross-beam energy transfer [12]. Conversely, beam 1 only had to be repointed by 2.80°. To minimize the repointing of beam 2, a solution was sought with intermediate repointings for each beam.

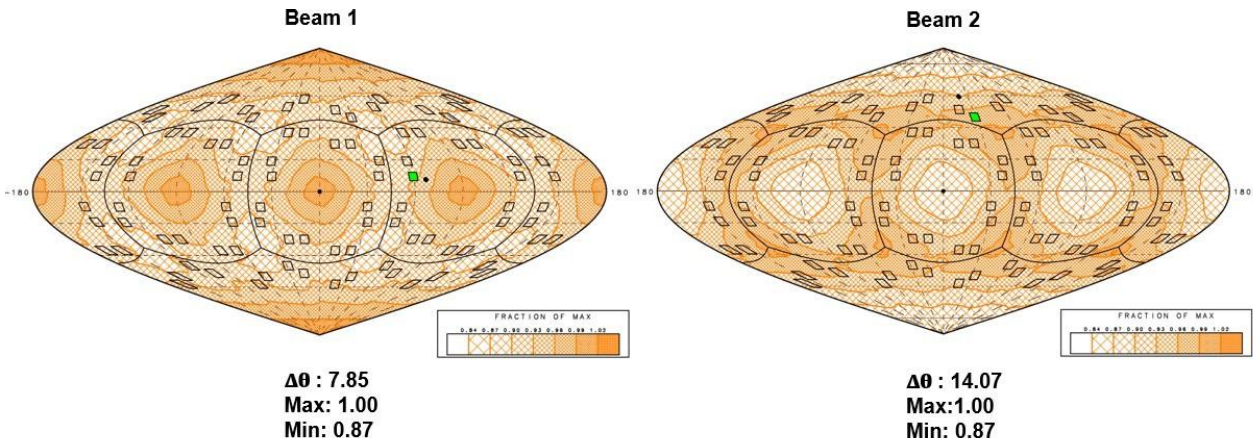


Figure 8: *Symmetrized energy deposition patterns for beam 1 (left) and beam 2 (right), for the final optimization. The two deposition patterns are complementary, with the same maximum (1.0) and minimum (0.87) values at different locations. This enables the maximum repointing angle Δθ of beam 2 to be reduced to 14.07°.*

To reduce the repointing angle of beam 2, beam 1 was pointed further from the ideal aim point toward the center of the face while beam 2 was pointed closer to the ideal aim point, producing the complementary deposition patterns shown in Fig. 8. These patterns ensure that when the two beams are combined, the strong center and weak corners of beam 1 line up with the weak center and strong corners of beam 2. As shown in Fig. 8, the maximum and minimum contours of beams 1 and 2 have the same values in complementary locations, allowing the deposition patterns, when combined, to have a low RMS while also lowering the repointing of beam 2 from 20.78° to 14.07°.

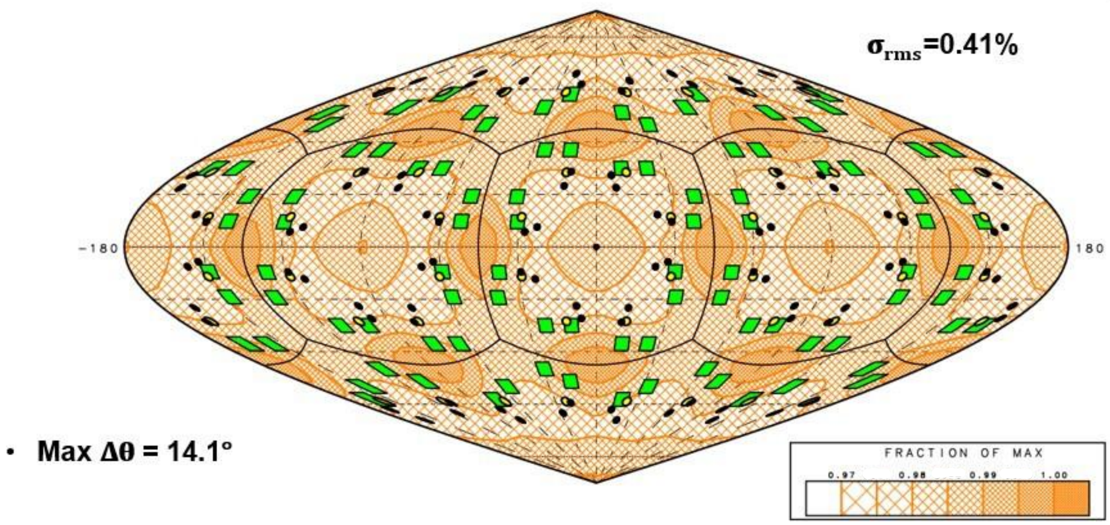


Figure 9: *Time-integrated energy deposition pattern for the final optimization of the 96-quad system with all 96 beams modeled. The yellow dots with black borders represent the ideal aim points and the black dots the optimized aim points.*

When the new complementary optimization of beams 1 and 2 is combined with the optimization of the other two beams, 49 and 50, the deposition pattern in Fig. 9 is achieved. For this figure, the optimized pointings of the four beams were applied to all 96 beams and the resulting deposition was also symmetrized, to ensure the most accurate model with numerical noise minimized. The scale is the same as for Fig. 7, with the lowest contour 0.97% of the maximum. The lowest value plotted is 0.98%, so although the deposition pattern has stronger edges and weaker corners, the overall variability is very low. Along with the maximum shift $\Delta\theta$ decreasing from 20.78° to 14.07°, the RMS has also decreased from the 0.51% in Fig. 7 to 0.41%.

## V  Conclusions

This work investigated the optimization of uniformity for direct drive experiments on a possible future laser facility that uses 96 quads. A key feature of the facility is that it can be used for both direct and indirect drive. Indirect drive will use spherical hohlraums with six laser entrance holes, which promise greater uniformity than the cylindrical hohlraums used on the

NIF. The 2-D hydrodynamics code *SAGE* was used to calculate beam repointings that provide maximum laser irradiation uniformity for direct drive. The optimum pointing design minimizes the repointing angles of the beams and results in a nonuniformity of 0.41% (RMS), with no beam repointed by more than 14.1° (compared with ~35° for direct drive designs on the NIF). These results show that the optimized design promises highly uniform direct drive implosions on a facility also capable of highly uniform indirect drive.

**Acknowledgments**

I would like to thank Dr. Craxton for all the hours he has dedicated to helping me do this research and for putting together this program. I would also like to thank my fellow students for their support. Additionally, the IT department was a great help through all the network issues I had. Lastly, I would like to thank Ms. Truebger for all her help in making sure this program ran smoothly.

**References**

[1] W. Wang. “Development of a Beam Configuration for the SG4 Laser to Support both Direct and Indirect Drive”. In: LLE Summer High School Research Program (2019). URL: https://www.lle.rochester.edu/media/publications/high_school_reports/documents/hs_reports/2019/Wang_William.pdf.

[2] J. D. Lindl. “Development of the indirect-drive approach to inertial confinement fusion and the target physics basis for ignition and gain”. In: Physics of Plasmas 2.11 (1995), pp. 3933-4024. DOI: 10.1063/1.871025. eprint: https://doi.org/10.1063/1.871025. URL: https://doi.org/10.1063/1.871025.

[3] P. B. Radha et al. “Direct drive: Simulations and results from the National Ignition Facility”. In: Physics of Plasmas 23.5 (2016), p. 056305. DOI: 10.1063/1.4946023. eprint: https://doi.org/10.1063/1.4946023.

[4] T. J. B. Collins et al. “A polar-drive-ignition design for the National Ignition Facility”. In: Physics of Plasmas 19.5 (2012), p. 056308. DOI: 10.1063/1.3693969. eprint: https://doi.org/10.1063/1.3693969. URL: https://doi.org/10.1063/1.3693969.

[5] K. Lan et al. “Octahedral spherical hohlraum and its laser arrangement for inertial fusion”. In: Physics of Plasmas 21.5 (2014), p. 052704. DOI: 10.1063/1.4878835. eprint: https://doi.org/10.1063/1.4878835. URL: https://doi.org/10.1063/1.4878835.

[6] K. Lan and W. Zheng. “Novel spherical hohlraum with cylindrical laser entrance holes and shields”. In: Physics of Plasmas 21.9 (2014), p. 090704. DOI: 10.1063/1.4895503. eprint: https://doi.org/10.1063/1.4895503. URL: https://doi.org/10.1063/1.4895503.

[7] K. Lan et al. “High Flux Symmetry of the Spherical Hohlraum with Octahedral 6 LEHs at the Hohlraum-to-Capsule Radius Ratio of 5.14”. In: Physics of Plasmas 21 (2014). DOI:

10.1063/1.4863435.

[8] S. A. Bel’kov et al. “Thermonuclear Targets for Direct-Drive Ignition by a Megajoule Laser Pulse”. In: Journal of Experimental and Theoretical Physics 121.4 (2015). ISSN: 1063-7761.

[9] N. N. Demchenko. “Uniformity Simulation of Multiple-Beam Irradiation of a Spherical Laser Target with the Inclusion of Radiation Absorption and Refraction”. In: Quantum Electronics 49.2 (2019). URL: https://doi/org/10.1070/QEL16784.

[10] M. Marangola. “Optimization of Direct Drive Designs for a Proposed Dual Direct/ Indirect Drive Laser”. In: LLE Summer High School Research Program (2021). URL: https://www.lle.rochester.edu/media/publications/high_school_reports/documents/hs_reports/2021/Marangola_Meghan.pdf.

[11] R. S. Craxton. “A Dual Laser-Beam Configuration Compatible with Both Symmetric Direct Drive and Spherical Hohlraums”. Presented at: 63rd Annual Meeting of the American Physical Society Division of Plasma Physics, Pittsburgh, PA, Nov. 2021.

[12] R.K. Kirkwood et al. “Observation of Energy Transfer Between Frequency-Mismatched Laser Beams in a Large-Scale Plasma”. In: Physical Review Letters 76.12 (1996), p. 2065. URL: https://doi.org/10.1103/PhysRevLett.76.